

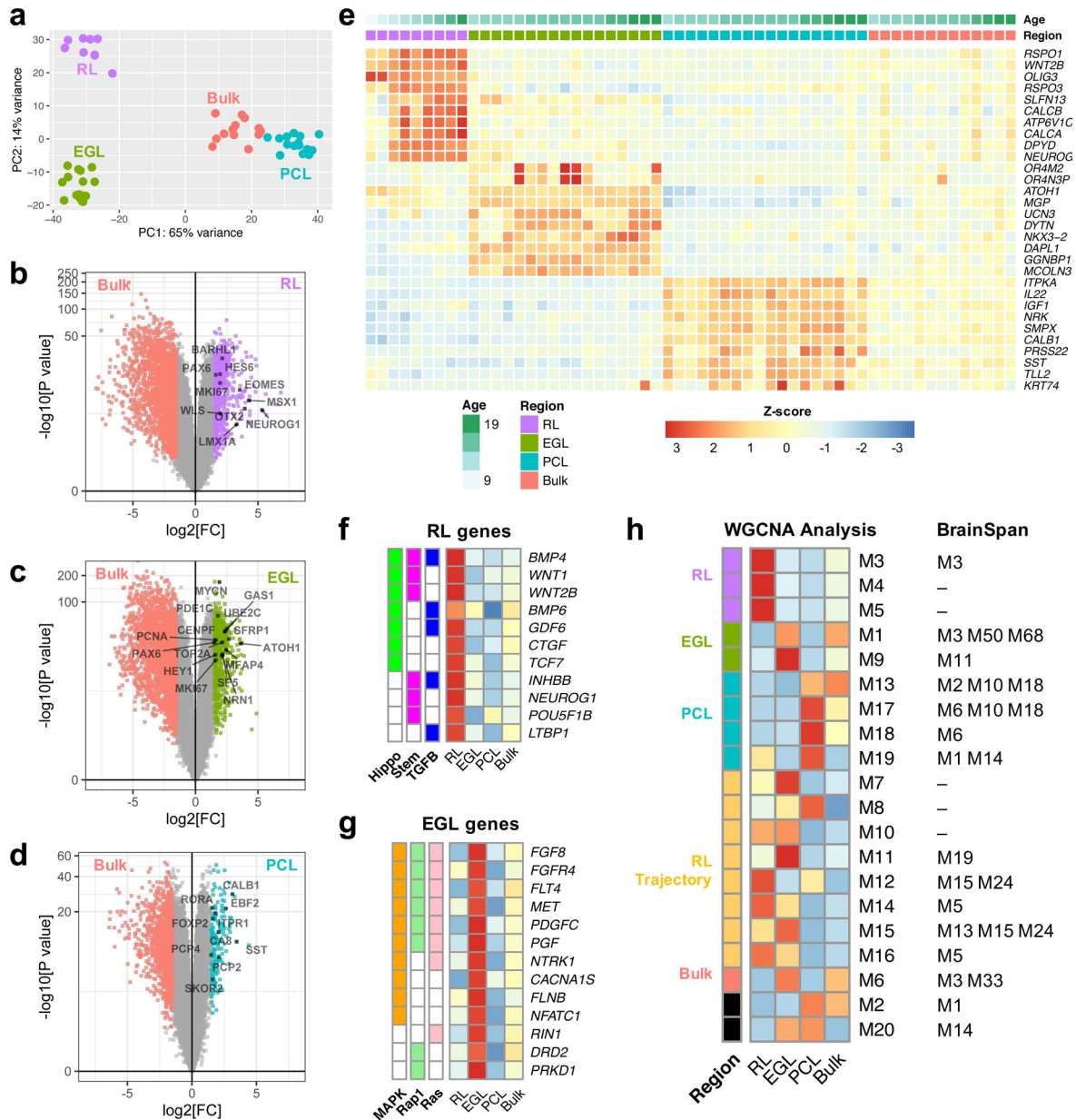
**Fig. 1 | Overview of prenatal cerebellar development and the data generated in this study.**

**a**, Midsagittal sections of the human fetal cerebellum stained with hematoxylin and eosin (H&E) or markers for Purkinje cells (Calbindin) or rhombic lip (RL) and external granule cell layer (EGL; PAX6 and KI67). A minimum of 2 samples per age were stained with adjacent sections used for histology and immunocytochemistry. The ventricular zone (VZ), RL, EGL, and Purkinje cell layer (PCL) are shown. Arrowheads mark the anterior (yellow) and posterior (white) EGL across the dorsal surface of the cerebellar anlage. At 9 PCW, the cerebellar anlage is dominated by Purkinje cells, with a thin nascent EGL extending from the RL. By 19 PCW, Purkinje cells have migrated radially to establish a multicellular layer (PCL) beneath the EGL. Scale bars: 100 um (grey), 500 um (red), 1 mm (blue). *10 PCW H&E section was used previously in Fig. 1 of Haldipur et al., 2019.*

**b**, Schematic illustrating the experimental workflow. N = 16 samples for Bulk RNA and Histology. N = 13 samples for LCM and SPLIT-seq. SPLIT-seq involves Pool, Split, and Pooling steps.

**c**, Timeline of cerebellar development from 9 to 21 PCW, with a summary of LCM and snRNA-seq samples. Legend: ● = sample present, ○ = sample absent.

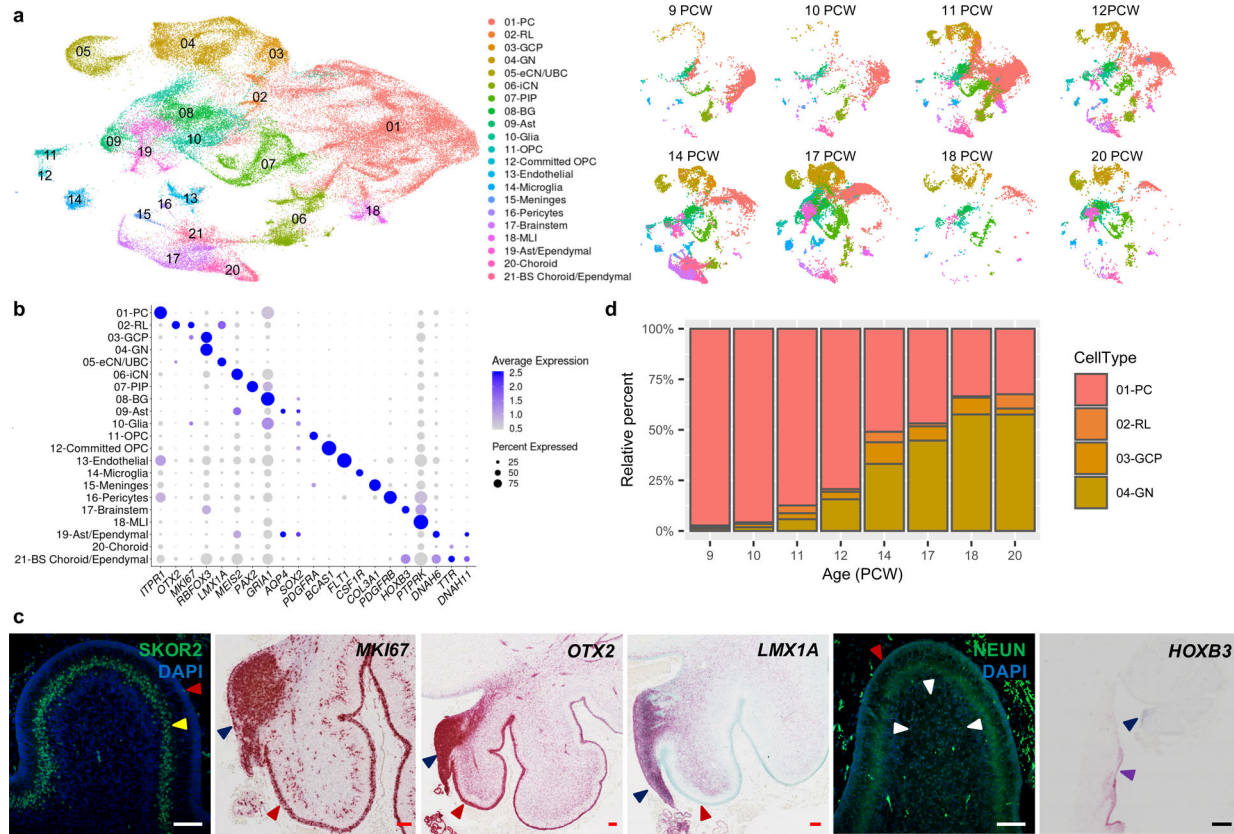
LCM (left) and SPLiT-seq (right) experimental workflows. **c**, The time span of fetal cerebellar development represented by line drawings of midsagittal sections of the cerebellum (to-scale) showing a dramatic change in size and foliation from 9 to 19 PCW. Below is the distribution of cerebella in this study. Biological and technical replicate samples are not shown (RNA-seq sample numbers: n = 13 for bulk; 9 for RL; 17 for EGL; 18 for PCL; snRNA-seq sample numbers: n = 6 for Exp 1; 11 for Exp 2; 9 for Exp 3).



**Fig. 2 |. Spatial transcriptional analysis of the developing human cerebellum.**

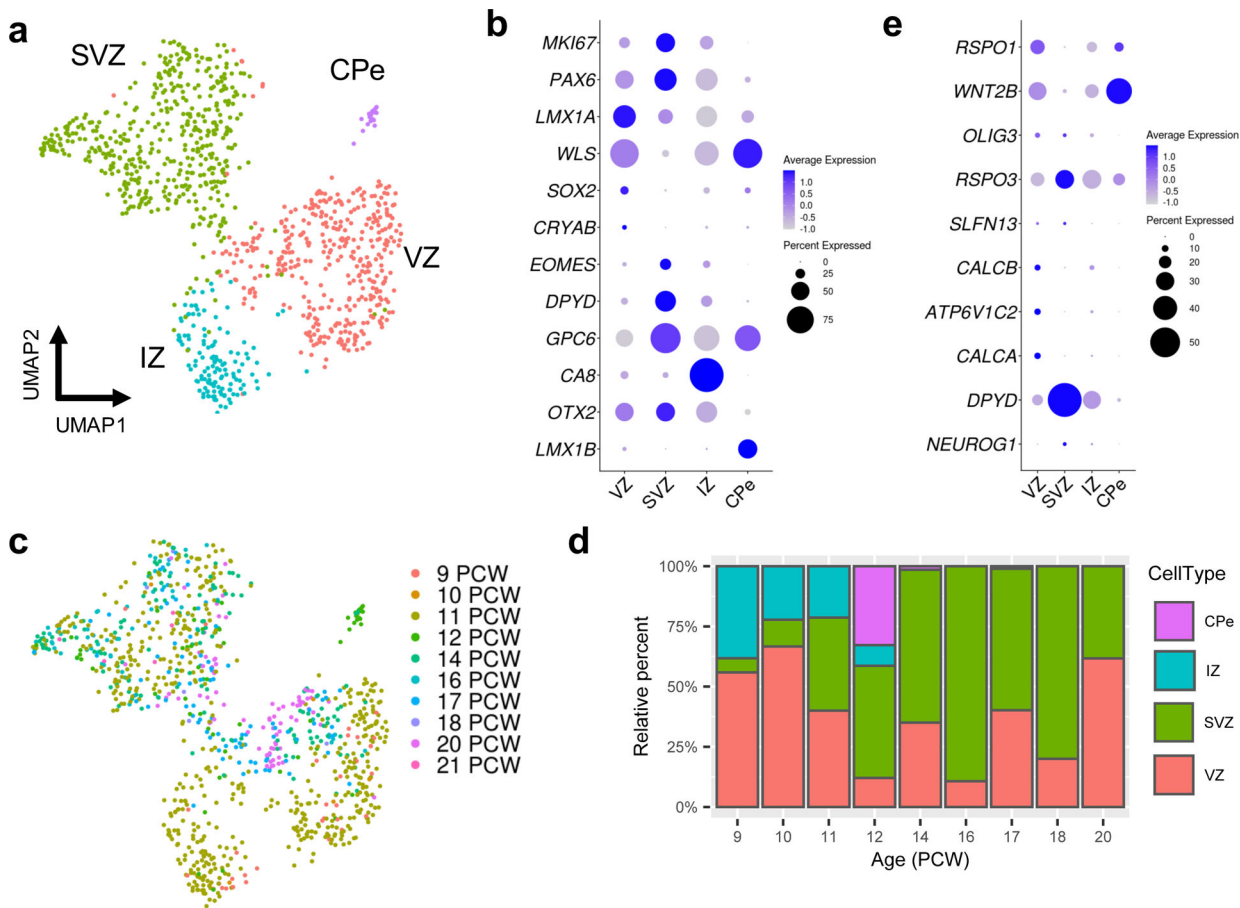
**a**, Principal component analysis indicates that the largest source of variation among RNA-seq samples was spatial location, accounting for 57% of the variance, and verifying LCM successfully captured these regions. **b-d**, Volcano plots illustrating differential expression of genes for each spatial region versus bulk cerebellum. Colored dots represent genes with significant expression [FDR<0.05; Log2(FC)>1.5]. Selected canonical genes with significant expression are labeled. Significance was determined by the Wald test and adjusted using FDR. Statistics are presented in Supplementary Table 3. **e**, Heatmap of the top 10 genes with significant expression per spatial region (RL, EGL, PCL) are shown for each sample. Samples are ordered by region [RL (purple), EGL (green), PCL (turquoise), bulk (salmon)], then by ascending age (9 to 19 PCW). High expression is in red and low

expression is in blue. **f,g**, Heatmaps of genes and pathways expressed in RL (f) and EGL (g) identified by gene ontology analysis. High expression is in red and low expression is in blue; Z-score legend as in **e**. Colored boxes indicate genes represented in enriched pathways: Hippo signaling (green), signaling pathways regulating pluripotency of stem cells (magenta), and Tgf $\beta$  signaling (blue) in **f**; MAPK signaling (orange), Rap1 (green), Ras (pink) in **g**. Statistics are presented in Supplementary Table 4. **h**, Heatmap of genes expressed in each WGCNA module enriched in **a**. High expression is in red and low expression is in blue; Z-score legend as in **e**. Colored boxes represent the cerebellar region interpretation for each WGCNA module, as in Supplementary Table 5.



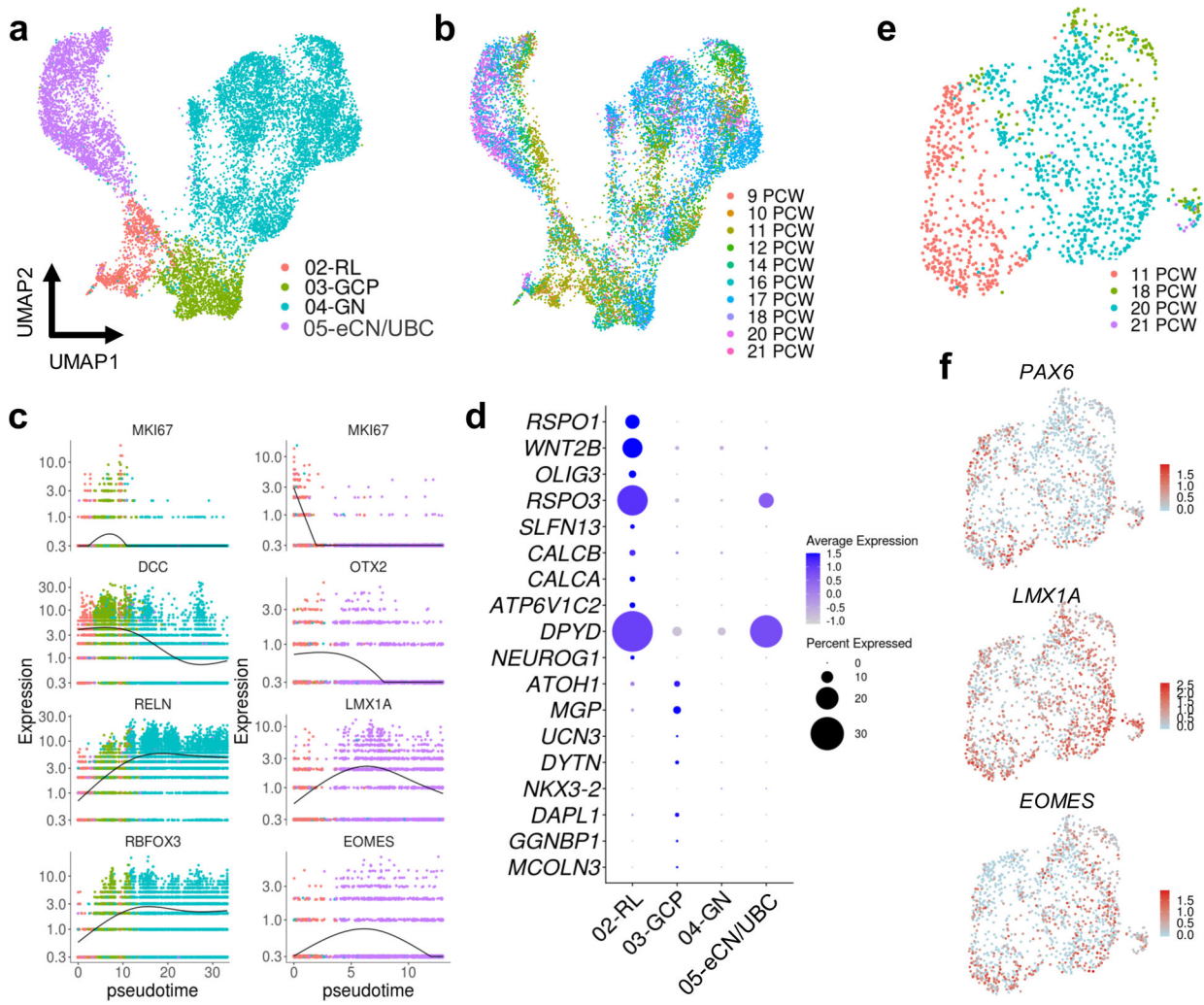
**Fig. 3 |. Identifying the major cell types of the developing human cerebellum.**

**a**, UMAP visualization of 67,174 human cerebellar nuclei colored by cluster identity from Louvain clustering and annotated on the basis of marker genes. The same UMAP is plotted at right, showing only nuclei from each age (nuclei numbers from left to right: n = 5,003 for 9 PCW; 2,329 for 10 PCW; 20,364 for 11 PCW; 7,119 for 12 PCW; 11,213 for 14 PCW; 15,556 for 17 PCW; 1,617 for 18 PCW; 5,177 for 20 PCW). **b**, Dot plot showing the expression of one selected marker gene per cell type. The size of the dot represents the percentage of nuclei within a cell type in which that marker was detected and its color represents the average expression level. Statistics are presented in Supplementary Table 9. **c**, Midsagittal sections of the human fetal cerebellum at 18 PCW stained with selected marker genes for Purkinje cells (SKOR2), proliferation (MKI67), RL (*OTX2* and *LMX1A*), granule neurons (NEUN), and brainstem (*HOXB3*). Adjacent sections from one sample were stained for *OTX2* and *HOXB3*; a minimum of 3 sections from each of 3 samples were stained for the other markers. The EGL, PCL, internal granule cell layer, RL and brainstem are indicated by red, yellow, white, blue and purple arrowheads, respectively. Sections are counterstained using DAPI for immunohistochemistry (SKOR2, NEUN) or Fast Green for *in situ* hybridization (MKI67, *OTX2*, *LMX1A*, *HOXB3*). Scale bar = 100 um and 1 mm (*HOXB3*). *LMX1A* was used previously in Fig. 3G of Haldipur et al., 2019. **d**, Stacked bar charts show the percentage of the four major cell types from each age sampled. Bar colors represent Purkinje cells (PC), rhombic lip (RL), granule cell precursors (GCP), or granule neurons (GN).



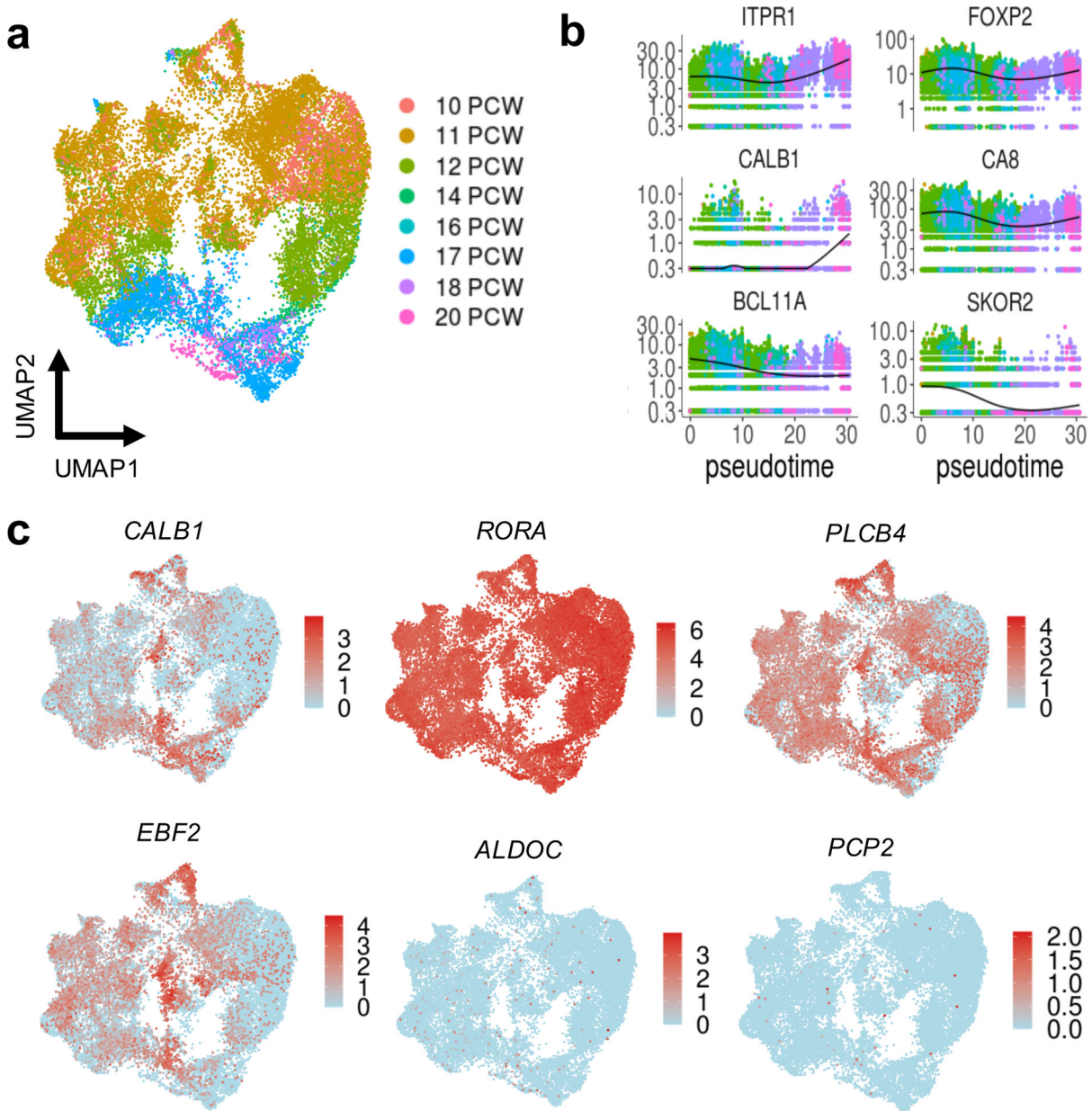
**Fig. 4 | Analysis of RL compartments at single-cell resolution.**

**a**, UMAP visualization and marker-based annotation of the RL subclusters ( $n = 1,018$  nuclei; 466 for SVZ; 390 for VZ; 135 for IZ; 21 for CPe). IZ, intermediate zone; SVZ, subventricular zone; VZ ventricular zone. **b**, Dot plot showing the expression of selected marker genes in subclusters. **c**, The same UMAP as in **a** with nuclei colored by sample age ( $n = 34$  for 9 PCW; 9 for 10 PCW, 535 for 11 PCW; 58 for 12 PCW; 137 for 14 PCW; 56 for 16 PCW; 97 for 17 PCW, 5 for 18 PCW; 81 for 20 PCW; 6 for 21 PCW). **d**, Stacked bar charts show the percentage of the RL subclusters by sample age. **e**, Dot plot showing the expression of the top 10 most differentially expressed genes from the spatial transcriptional analysis of the RL (Fig. 2e and Supplementary Table 3).

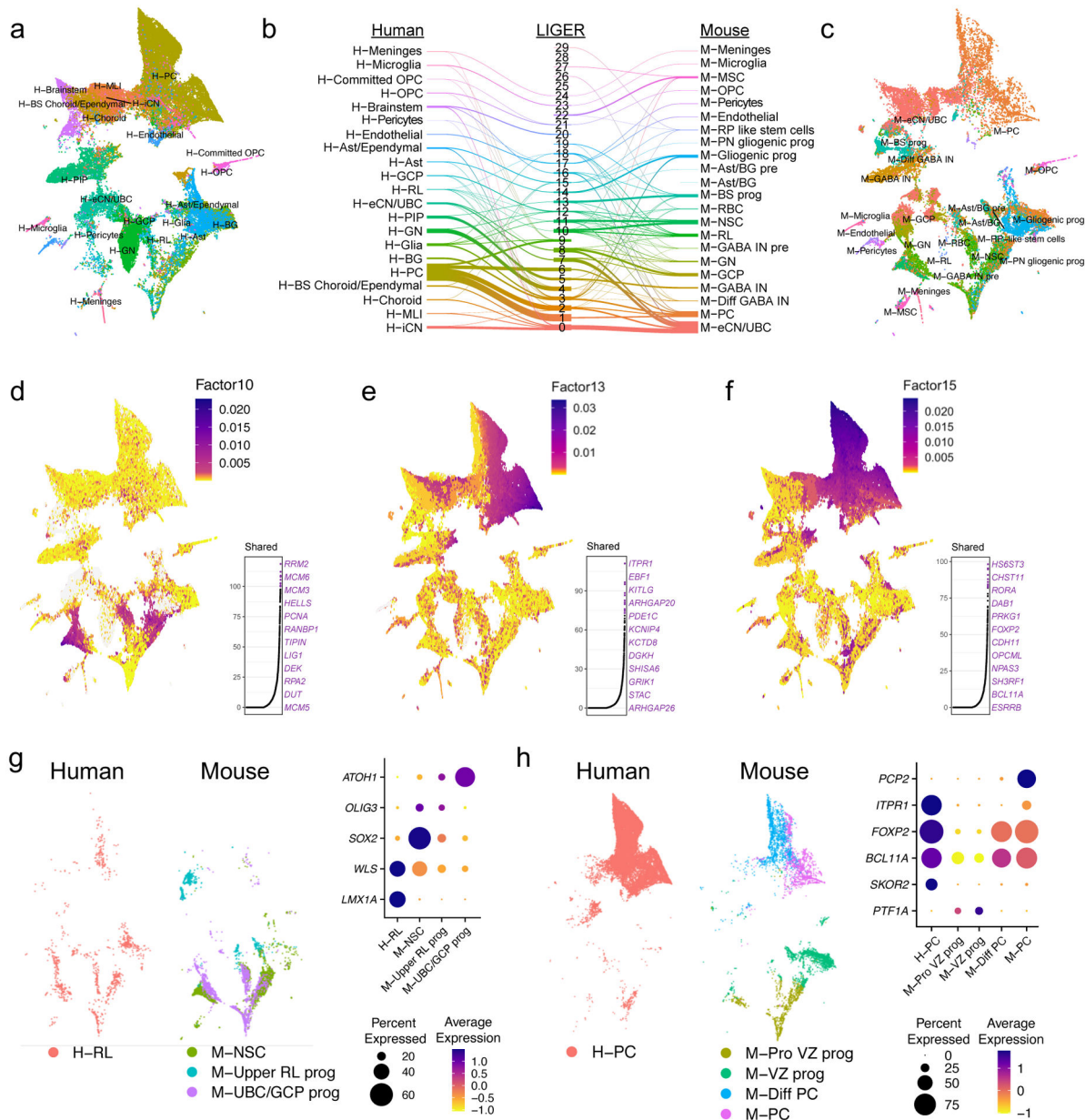


**Fig. 5 | Characterization of the RL trajectory.**

**a**, UMAP visualization and marker-based annotation of cell types that originate from the RL ( $n = 12,243$ ; 1,018 for RL; 1,659 for GCP; 6,727 for GN; 2,839 for eCN/UBC). eCN/UBC, excitatory cerebellar nuclei/unipolar brush cells; GCP, granule cell progenitors; GN, granule neurons; RL, rhombic lip. **b**, The same UMAP as in **a** with nuclei colored by sample age ( $n = 120$  for 9 PCW; 61 for 10 PCW; 2,190 for 11 PCW; 1,053 for 12 PCW; 1,663 for 14 PCW; 432 for 16 PCW; 4,410 for 17 PCW; 627 for 18 PCW; 1,626 for 20 PCW; 89 for 21 PCW). **c**, Kinetics plot showing the relative expression of RL trajectory marker genes across developmental pseudotime. Dots are colored according to cell types as in **a**. **d**, Dot plot showing the expression of the top 10 most differentially expressed genes from the spatial transcriptional analysis of RL and EGL (Fig. 2e and Supplementary Table 3). **e**, UMAP visualization of the eCN/UBC cluster including 11, 18, 20, 21 PCW samples. Nuclei are colored by sample age ( $n = 1,424$ ; 436 for 11 PCW; 138 for 18 PCW; 842 for 20 PCW; 8 for 21 PCW). **f**, The same UMAP as in **e** with nuclei colored by expression level for the indicated gene.

**Fig. 6 |. Purkinje cells.**

**a**, UMAP visualization of the PC cluster. Nuclei are colored by sample age ( $n = 25,724$ ; 3,736 for 9 PCW; 1,131 for 10 PCW; 12,182 for 11 PCW; 3,543 for 12 PCW; 1,346 for 14 PCW; 26 for 16 PCW; 3,144 for 17 PCW; 245 for 18 PCW; 371 for 20 PCW). **b**, Kinetics plot showing the relative expression of PC marker genes across developmental pseudotime. Dots are colored by sample age as in **a**. **c**, The same UMAP as in **a** with nuclei colored by expression level for the indicated gene.

**Fig. 7 |. Human-mouse cross-species analysis.**

**a**, UMAP plot of nuclei from human cerebellum and cells from mouse cerebellum following LIGER analysis, showing only nuclei from human cerebellum ( $n = 69,174$ ) and colored by cell type from the original analysis. **b**, Riverplot showing the relationship between original cluster assignments from our human cerebellum and a published mouse cerebellum dataset. **c**, UMAP plot of nuclei from human cerebellum and cells from mouse cerebellum following LIGER analysis, showing only cells from mouse cerebellum ( $n = 39,130$ ) and colored by cell type from the original analysis. **d-f**, UMAP plots showing cell factor loading values and gene loading plots for factors corresponding to RL (**d**, and PC (**e**, **f**). **g**, UMAP plots show the human ( $n = 1,018$ ) and mouse (7,034) cell types contributing to factor 10. Dot plot shows expression of canonical RL genes delineated in human and mouse clusters. **h**, UMAP plots

show the human and mouse PC clusters. Dot plot shows expression of canonical PC genes delineated in human and mouse PC clusters.

Author Manuscript

Author Manuscript

Author Manuscript

Author Manuscript

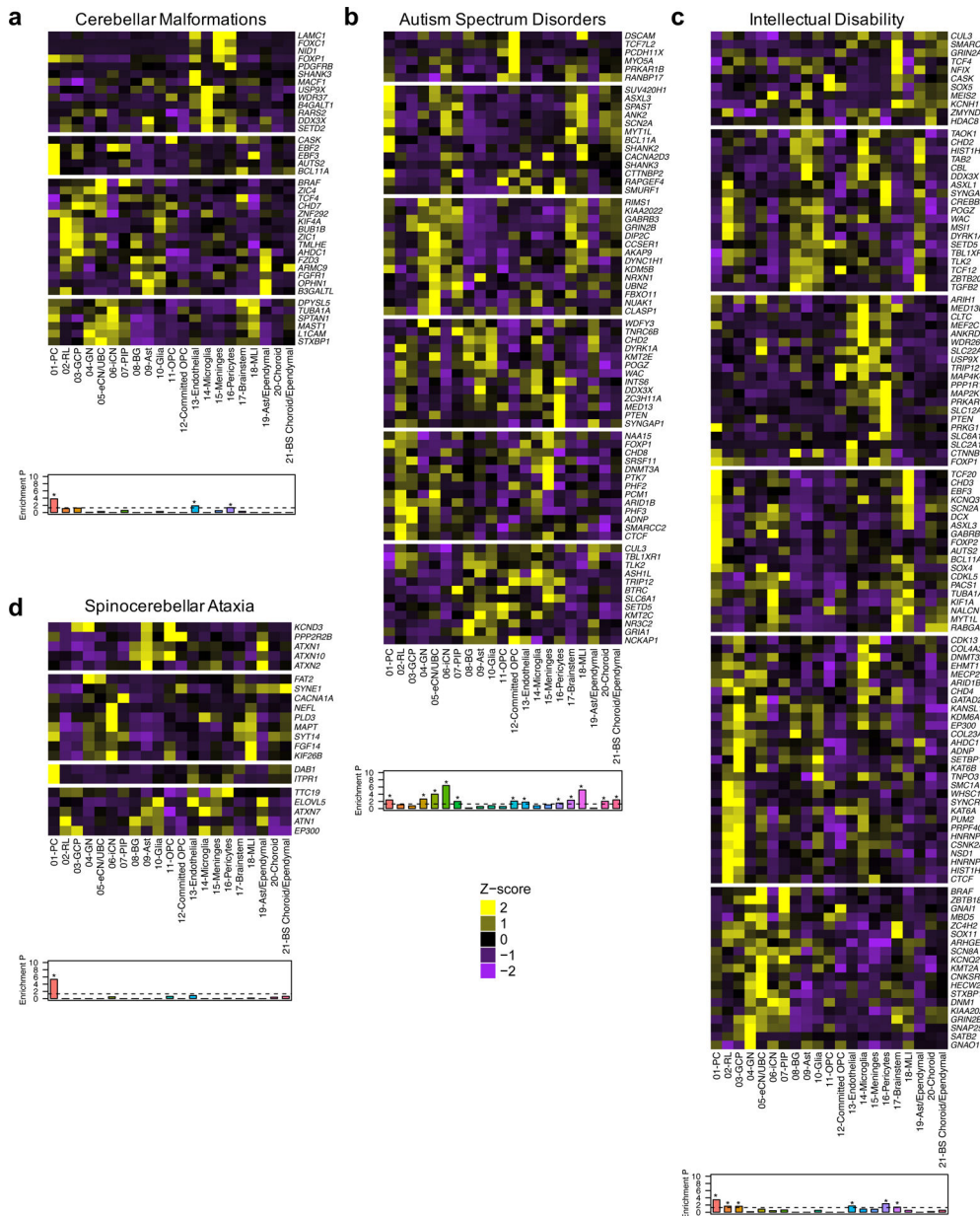


**Fig. 8 |. Cerebellar cell type enrichment in pediatric and adult diseases.**

**a-d**, Heatmaps of mean expression per fetal cerebellar cell type for genes associated with pediatric (**a**, cerebellar malformations; **b**, autism spectrum disorders; **c**, intellectual disability) or adult (**d**, spinocerebellar ataxia) diseases. Color scheme is based on Z-score distribution. In the heatmaps, each row represents one gene and each column represents a single cell type. Gene expression was clustered by row. Horizontal white lines indicate branch divisions in row dendograms (not shown). The full list of genes is provided in Supplementary Table 11. Enrichment *P* values (-Log<sub>10</sub> *P* value) for each cell type are shown in the bottom bar plots. Significance was determined by one-sample Z-test, two-tailed *P* value. The dashed line is the significance threshold. Asterisk (\*) indicates significance (*P* < 0.05) after Bonferroni correction: cerebellar malformations (*P* = 1.63 × 10<sup>-4</sup> for 01-PC; 0.01

for 13-Endothelial; < 0.05 for 16-Pericytes), autism spectrum disorders ( $P=0.004$  for 01-PC; 0.002 for 04-GN;  $9.43 \times 10^{-5}$  for 05-eCN/UBC;  $3.78 \times 10^{-7}$  for 06-iCN; 0.01 for 07-PIP; 0.008 for 12-Committed OPC; 0.02 for 13-Endothelial; 0.03 for 16-Pericytes; 0.005 for 17-Brainstem;  $6.74 \times 10^{-6}$  for 18-MLI; 0.009 for 20-Choroid; 0.004 for 21-BS Choroid/ependymal), intellectual disability ( $P=3.30 \times 10^{-4}$  for 01-PC; 0.02 for 02-RL; 0.02 for 03-GCP; 0.02 for 13-Endothelial; 0.004 for 16-Pericytes; 0.04 for 17-Brainstem), spinocerebellar ataxia ( $P=4.56 \times 10^{-6}$  for 01-PC).